Soft Matter

Cite this: *Soft Matter*, 2011, **7**, 3177

www.rsc.org/softmatter

PAPER

Defect hydrodynamics in 2D polar active fluids†

J. Elgeti,[a] M. E. Cates[b] and D. Marenduzzo[b]

Received 4th October 2010, Accepted 18th January 2011
DOI: 10.1039/c0sm01097a

We present a systematic analysis of the phase diagram of a defect in an active polar fluid, found by means of Lattice Boltzmann simulations. We show that for rod-like active particles, extensile activity favours spirals and contractile activity favours asters. Polarity on the other hand introduces "self-advection terms" which can change the relative stability of defects quite dramatically. We also study the interactions of two nearby defects and uncover a novel and very rich phenomenology, which includes spontaneous rotation and oscillations for extensile activity. We discuss the possible relevance of our results to concentrated microbial suspensions and microtubular networks *in vitro*.

1 Introduction

Active fluids and active gels have by now become a topical area of research. Generally speaking, an active particle "absorbs energy from its surroundings or from an internal fuel tank and dissipates it in the process of carrying out internal movements".[1] This definition applies to bacteria, swimming algae and other microorganisms,[2] as well as to living cells or cell extracts.[3–5] However active materials may also be non-biological, and a synthetic example is a shaken granular fluid.[6] As the definition clearly implies, active materials may remain far from thermodynamic equilibrium even in steady state, due to their continuous energy intake, and this renders their properties of particular interest to physicists.

Active particles also continuously exert forces on their surrounding fluid, and it is indeed this "stirring" which leads to many unexpected features in their physics. As there is no external force on an active particle such as a swimming microorganism, if we neglect gravity which is usually small, the simplest force field which an active particle can exert is a dipole. If the direction of the forces is from the centre of mass of the particle to the fluid, the particle is "extensile", or a "pusher", otherwise it is "contractile", or a "puller".[7,8] Being extensile or contractile leads to vastly different responses and physics, as has been shown several times in the literature—this property will also be crucial to our work. Examples of extensile active fluids are most bacterial suspensions such as *B. subtilis* films, whereas *Chlamydomonas* is contractile, as are actomyosin solutions.[4,9]

A further crucial properties of many active fluids is that they are intrinsically polar. For instance, myosin performs a directed walk from the minus to the plus end of cytoskeletal fibers, and bacteria break the symmetry by swimming. Individual polar and apolar active particles are sometimes referred to as "movers" and "shakers" respectively.[1] On one hand, even concentrated suspensions of movers may well form globally apolar phases, for instance when there are on average the same number of particles moving one way or another. However, to completely describe a generic active fluid one should allow for a polar order parameter—the simplest of which is a vector whose magnitude is variable and sharply drops or vanishes at defects, or in the isotropic phase.[10,11] Here we therefore follow this procedure and single out the effect of purely polar terms in our simulations, at variance with previous 2D numerical work which mainly considered apolar fluids.[12]

A particularly successful way to describe active fluids is to coarse grain over the details of the microscopic model and write down a set of hydrodynamic equations of motion. These show a remarkable degree of universality, and they can be written down phenomenologically on the basis of the underlying symmetries alone.[1,13] Analytical and computational work on these hydrodynamic equations has already shown that active fluids can exhibit a range of interesting and unexpected behaviours which have no counterpart in the hydrodynamics of passive fluids in thermodynamic equilibrium. For instance, active fluids may spontaneously flow in the steady state without external forcing, provided their activity is sufficiently large. In extensile active fluids, spontaneous flow in 2D may also become effectively chaotic or turbulent, resembling experiments on thin films which monitor the onset of large scale vortices and of the so-called "bacterial turbulence", in *e.g. B. subtilis* films.[14–16] The rheology of active fluids is also strikingly non-trivial, with activity-induced thinning and thickening in the non-linear response of these fluids to an imposed shear or pressure gradient.[17,18]

Here we focus on the steady state and dynamic properties of defects in a 2D active fluid. We work in a geometry in which there is an active circular region surrounded by a passive isotropic

[a]*Physical Chemistry Unit (UMR 168, CNRS UPMC), Institut Curie, Paris, 75248, Cedex 5, France*
[b]*SUPA, School of Physics and Astronomy, University of Edinburgh, Edinburgh, EH9 3JZ, UK*
† Electronic supplementary information (ESI) available. See DOI: 10.1039/c0sm01097a

background. Our main aim in this paper is to map out the full phase diagram for a single defect in an active fluid, as a function of the magnitude and sign of the activity parameters entering the hydrodynamic theory. Broadly, we find that, for solutions of rod-shaped particles, contractile activity tends to favour aster-like defects whereas extensile activity more often leads to rotating spirals or vortices. Remarkably, we find stable steady states even for "tumbling" fluids, which never settle under a shear flow in the case of a passive liquid crystal. Polarity on the other hand leads to an effective self-advection which changes the phase diagram significantly.

Our second objective in this work is to initiate the study of the hydrodynamic interaction between (two) nearby defects in an active fluid. We find that these give rise to a rich dynamical behaviour. Extensile spirals may oscillate or continuously rotate around each other, while contractility leads to a stable steady state with coexisting asters with opposite polarities. Our results suggest that it would be interesting to study experimentally the motion of topological defects in bacterial or microbial fluids.

2 Model and methods

In this work, we want to study the hydrodynamics in an active polar fluid. Accordingly, we describe the order *via* a vector **P** (with variable magnitude), which we call the polarisation field. This ensures that there is no head-tail symmetry in the system, as opposed to the case of standard, passive nematic liquid crystals, where the order parameter is a second rank tensor.[19]

The equations of motion we used in our LB simulations are a simplified version of those presented in ref. 10, 11 mainly because in our situation we consider the density to be constant. In the limit in which we consider a purely apolar active fluid, we recover the hydrodynamic model proposed by Voituriez *et al.*[20–22] and equivalent to that originally presented by Kruse *et al.*[4]

The equation governing the evolution of the vectorial order parameter is

$$[\partial_t + (v_\beta + wP_\beta)\partial_\beta)]\ P_\alpha = \lambda D_{\alpha\beta}P_\beta - \omega_{\alpha\beta}P_\beta + \Gamma' h_\alpha. \qquad (1)$$

In this equation, **v** is the velocity field, $\omega_{\alpha\beta}$ and $D_{\alpha\beta}$ are the antisymmetric and symmetric part of the tensor $\partial_\alpha v_\beta$, whereas w is an active term, due to swimming, which causes *self-advection* of the order parameter. Furthermore, h_α is the "molecular field" (defined below), Γ' is a relaxation constant related to the rotational viscosity of the active liquid crystal, and λ is a material dependent constant—positive for rod-like molecules and negative for disc-like ones. If $|\lambda| > 1$ the liquid crystalline passive phase is flow-aligning, otherwise it is flow-tumbling. In a passive liquid crystalline fluid with no anchoring at the boundaries, flow-tumbling means that in an imposed steady shear the director field continuously rotates. Note also that Greek indices denote Cartesian coordinates and we use the Einstein convention that summation over repeated indices is implied. Finally note that our constant density approximation is likely to work better for the case $w = 0$, as suggested by the simulations in ref. 10 which showed an essentially constant concentration field in that case, whereas significant density variations were observed when self-advection was added. For simplicity, and to aid comparison of the cases we consider, we keep this constant density approximation in the $w \neq 0$ case—this should correspond to choosing a large free energy cost for density inhomogeneities in the language of ref. 10.

The "molecular field" is given by

$$h_\alpha = -\delta\mathscr{F}_{\mathrm{pol}}/\delta P_\alpha, \qquad (2)$$

where $\mathscr{F}_{\mathrm{pol}}$ is the free energy for a polar active nematic, whose density f is taken as (see also ref. 10 where a more general form is used):

$$f = \frac{a}{2}|\mathbf{P}|^2 + \frac{b}{4}|\mathbf{P}|^4 + \frac{K}{2}(\partial_\alpha P_\beta)^2 + \delta\frac{K}{2}(\varepsilon_{\alpha\beta\gamma}\partial_\beta P_\gamma)^2, \qquad (3)$$

where K and $K + \delta K$ are the splay and bend elastic constants (in a pure 2D geometry twist is irrelevant), $\varepsilon_{\alpha\beta\gamma}$ is the Levi–Civita (or permutation) tensor, $b > 0$, and we chose $a = -b$ to ensure that the minimum of the free energy is at $|\mathbf{P}| = 1$.

The velocity field, **v**, obeys both the continuity equation and the Navier–Stokes equation, which for effectively incompressible fluids reads

$$\rho[\partial_t + v_\beta\partial_\beta]v_\alpha = \partial_\beta\Pi_{\alpha\beta} + \eta\partial_\beta(\partial_\alpha v_\beta + \partial_\beta v_\alpha), \qquad (4)$$

where η is the viscosity, and $\Pi_{\alpha\beta}$ is a thermodynamic stress tensor, explicitly given by:

$$\Pi_{\alpha\beta} = \frac{1}{2}(P_\alpha h_\beta - P_\beta h_\alpha) - \frac{\lambda}{2}(P_\alpha h_\beta + P_\beta h_\alpha) - \zeta P_\alpha P_\beta \qquad (5)$$

As mentioned previously, the active term in the stress tensor, proportional to ζ, has therefore the same form for apolar and polar active gels (if the latter are represented by a headless vector $\sqrt{q}\mathbf{n}$, with q a scalar order parameter).

The equations of motion of the active polar fluids are solved by means of a hybrid lattice Boltzmann (LB) scheme,[23] which combines an LB treatment for the Navier–Stokes (and the continuity) equation with a standard finite difference algorithm to solve the order parameter dynamics. This method was previously used to study mainly tensorial order parameter dynamics, and some of the results which can be obtained with it were recently reviewed in ref. 24. It has also been used to study the hydrodynamics of binary fluids.[25] For a different way to treat the equations of motion of passive nematics numerically, see *e.g* ref. 26.

If we were to do simulations in a single phase with periodic boundary conditions, these would lead to an effective defect–defect interaction which we wish to avoid. Therefore, we instead study a "binary" system, in which an active circular patch of fluid, with radius R and polar ordering inside, is immersed in an isotropic and passive matrix. In order to realise this biphasic system, we implement a hybrid LB code where ζ (in eqn (5)) and a (in eqn (3)) are space dependent, and result in an active polar nematic droplet inside an isotropic background. To this end, we impose $\zeta = 0$ and $a = b$ outside the active patch, whereas $a = -b$ and $\zeta \neq 0$ inside it. A similar procedure was used in ref. 27 to study, within a tensorial approach, one or more active *apolar* nematic stripes or droplets inside a passive nematic background. Our choice may be seen as providing effectively free boundary conditions at the edge of the droplet. The magnitude of the polarisation field needs to vanish outside the droplet, while its direction is not specified at its boundary.

Note that we consider a 2D system, so that the polarisation vector in the ordered case, where it is of approximately constant magnitude, may be described by the angle with respect to the x axis, say ϕ. Furthermore, stable defect with topological charge equal to 1, which we focus on in Section 3.1, are best described in the polar (r, θ) coordinate system. For these cases, it is useful to represent the polarisation $\mathbf{P}$ in the polar coordinates,[4] with components

$$P_r = |\mathbf{P}|\cos - (\psi)$$
$$P_\theta = |\mathbf{P}|\sin - (\psi). \quad (6)$$

Equivalently, the Cartesian components of $\mathbf{P}$ are

$$P_x(r,\theta) = |\mathbf{P}|\cos - (\psi + \theta)$$
$$P_y(r,\theta) = |\mathbf{P}|\sin - (\psi + \theta). \quad (7)$$

(Note that in the equation above $\phi = \psi + \theta$).

Following the notation in ref. 4 and 5, we describe these defects *via* the angle ψ just defined in eqn (6). Configurations with ψ constant and equal to either 0 or π correspond to asters, whereas configurations with $\psi \equiv \pm\pi/2$ correspond to vortices. These are the only stable defects in polar (*e.g.* ferroelectric) passive liquid crystals. Spiral defects are metastable—they are characterised by a constant $\psi \equiv \psi_0$ within a one elastic constant model ($\delta K = 0$) and by a spatially varying ψ in general‡. In active polar liquid crystals, spirals are predicted to exist as stable states in selected regions of the parameter space.[4,5]

Note that in the following we will quote numbers in simulation units. While the qualitative trends are generic for several values of K and ζ, one may link our units to physical ones by assuming that we are modelling a patch of about 1 μm, and an active liquid crystal with a rotational viscosity of 1 Poise, in which case a value of K equal to 1 corresponds to 40 pN, while one space and time unit correspond to 0.02 μm and 1 μs respectively. One should bear in mind that mapping to specific biophysical systems may lead to very different conversions though; these values are based on those for conventional synthetic liquid crystals.

3 Results

3.1 Single defect: phase diagram

In this section we consider a single defect in the active circular patch. In the passive case, this defect would stay immobile and not leave the system as the single-defect state is metastable.

As a useful starting point, we simulated the case of an active liquid crystalline fluid with $\lambda < 0$ (this choice in the continuum equation correspond to an underlying fluid of disc-like particles), which was that previously considered in ref. 4. As an initial condition, in this and in all single-defect simulations reported in this section, for $|\lambda| > 1$ we took an inward pointing spiral with $\psi = \pi - \text{acos}(1/\lambda)/2$, which is the stable state predicted by the theory of ref. 4 in this regime. For $|\lambda| < 1$, instead we chose an outward pointing aster. Note that some noise is added to the initial condition to avoid trapping in metastable states.

For each of the steady state configurations which we find, we fit the polarisation field with the one of a spiral with fixed angle, see eqn (6) and ref. 4. The optimal fit then defines the "average" angle ψ_0 denoting the state. Below we show contour plots of $\cos\psi_0$. We still refer to these as "phase diagrams" and we identify asters as configurations with $|\cos\psi_0| > 0.9$, vortices as configurations with $|\cos\psi_0| < 0.1$, whereas we refer to all other states as spirals. Strictly speaking, then, with these definitions the boundaries should be thought of as typically denoting a crossover rather than a phase transition (there are some exceptions to this general rule, detailed below).

Fig. 1 shows the phase diagram which we obtain for $\lambda = -2$ (other parameters are given in the caption). We find three different "phases", a vortex, an aster and a spiral phase. At $\zeta = 0$, as expected, one can only observe a stable vortex or aster. The aster is stable over the vortex for $\delta K > 0$, *i.e.* when $K_3 > K_1$ so that splay deformations cost less than bend deformations. Note that this case is typical in standard (passive) liquid crystal solutions. As predicted in ref. 4, we find that a sufficiently contractile activity turns both asters and vortices into spirals, which are not stable in the absence of activity. The boundary between these "phases" are in good quantitative agreement with the ones predicted with linear stability analysis.[4] Furthermore, our LB simulations show that there is an additional crossover between asters and vortices, which is not at $\delta K = 0$ but occurs at positive δK for extensile active fluids.

Having validated our algorithm, we now proceed to systematically analyse how the phase diagram is modified with different values of the parameters. We will focus on the effects of λ and of the active *self-advection* term w.

3.1.1 Role of λ. To address the role of λ we firs set $w = 0$. Fig. 2 shows a typical phase diagram obtained for a flow-aligning suspension of rod-like particles ($\lambda = 2.1$). It can be seen that now spirals occur for extensile active fluids. These spirals

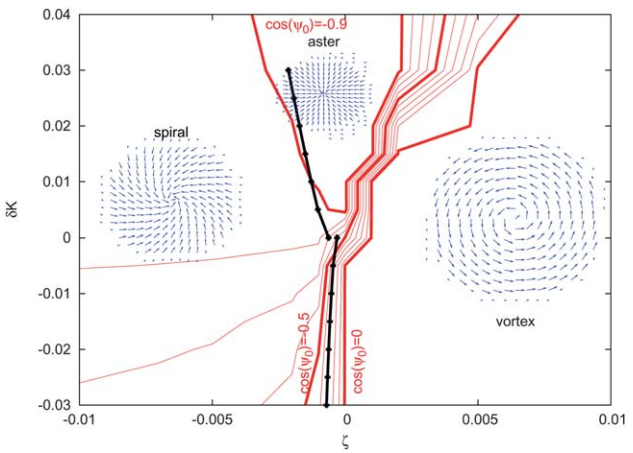

Fig. 1 Phase diagram in the $(\zeta, \delta K)$ plane of an active fluid with $\lambda = -2$ (therefore with disc-like constituents). Other parameters were: $b = -a = 0.1$, $\Gamma = 1$, $K = 0.04$, $\eta = 5/3$. Red lines are contour lines of $\cos\psi_0$. Starting from the top and going in a clockwise direction, thick lines correspond to $\cos\psi_0$ equal to -0.9, -0.5, 0, while thin lines correspond to increment of -0.1 each (*i.e.* from the top thin lines correspond to $\cos\psi_0$ equal to -0.8, -0.7, -0.6, -0.4, -0.3, -0.2, -0.1). The black lines denote the phase boundary between spirals and asters, and between spirals and vortices, as predicted in ref. 4.

‡ As our system is invariant under the transformation $\psi \rightarrow -\psi$, we present results in terms of $\cos(\psi)$.

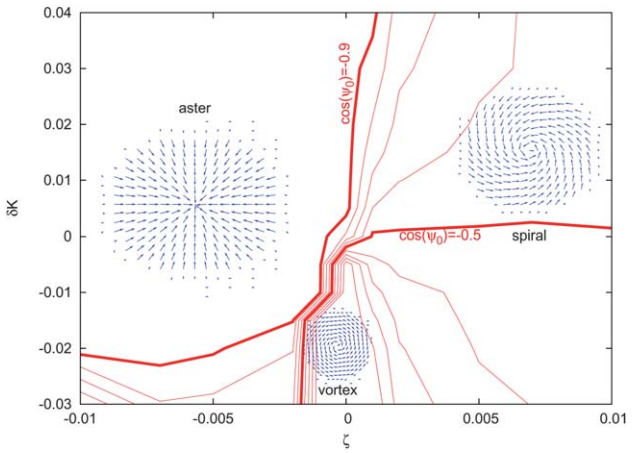

Fig. 2 Phase diagram with $\lambda = 2.1$, and other parameters as in Fig. 1. Thick red lines correspond to the values of $\cos\psi_0$ shown. Thin red lines correspond to successive differences of -0.1 in $\cos\psi_0$.

spontaneously flow, as is discussed more in detail below, which is in line with the result that in 1D systems extensile fluids undergo a linear instability to a spontaneously flowing state. Also, simulations of apolar inhomogeneous active nematic droplets in passive nematics showed spirals for extensile activity,[27] although no systematic analysis as the one presented here was previously attempted numerically. Suspensions of contractile flow-aligning active rods typically form asters, on the other hand, with vortices living close to the boundary between these two phases, and only existing for $\delta K < 0$.

The value of ψ_0 as a function of activity for different values of δK is shown in Fig. 3. This plot suggests that the crossover between asters to spirals for extensile fluids is very smooth, whereas the one between vortex and spirals is more abrupt for contractile suspensions. Actually, in some of these cases we see that there are finite activity windows for which $\cos\psi_0$ equal to 0 and -1, so that one may speak of a real non-equilibrium phase transition in these cases. Note that the information regarding the continuous or discontinuous character of a transition cannot be obtained from linear stability analysis, hence is a useful further theoretical prediction coming from simulations. The nature of the transition between these different kinds of defects could be tested in experiments which vary the concentration of a bacterial suspension or an actomyosin solution.

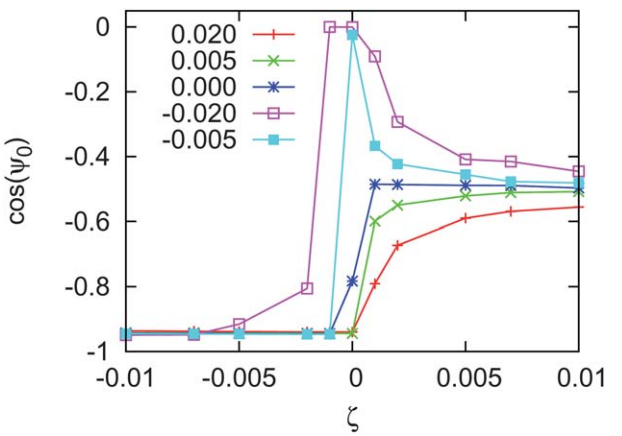

Fig. 3 Value of the angle ψ_0, see text, as a function of ζ, for different values of δK (see legend), and for $\lambda = 2.1$.

To further quantitatively describe the spirals obtained with our LB simulations, we show in Fig. 4 the spatial (radial) dependence of the angle ψ (as a splined average of the function ψ computed at all lattice points). We focused on data for $\zeta = 0.005$, *i.e.* an extensile fluid, for which we observed stable spirals in steady state. As mentioned above, from the theory we expect that ψ should be constant for $\delta K = 0$—this we find, apart from a small region close to the defect core. On the other hand, for $\delta K \neq 0$ the theory of ref. 4 shows that ψ *cannot* be constant, although an explicit analytical determination of its spatial dependence is not possible. Our results for $\delta K \neq 0$ show that in this case ψ does depend on r, but this function is rather flat apart from the regions close to the defect core and the boundary of the active patch.

As explained in ref. 4, spirals should rotate. To prove that this is the case and quantify the extent of the velocity field $\mathbf{v}$ in steady state, we plot in Fig. 5 the magnitude of this quantity as a function of the distance from the centre of the defect, r, for $\delta K = 0$ and different values of the activity. As expected, there is a finite steady state velocity which is associated to the rotation of the spiral. This spontaneous flow has the shape of a single vortex centred at $r = 0$. It is also interesting to observe that our active patch framework effectively leads to a no-slip velocity boundary condition at its edge.

All these results pertained to flow-aligning fluids. While these are the most natural case to study, at least based on the analogy to passive liquid crystals where they are the rule, experience from spontaneous flow results suggests that flow-tumbling fluids may lead to a significantly different phenomenology.[11,12,28,29] Therefore in Fig. 6 we present here a phase diagram for $\lambda = 0.7$, which corresponds to a flow-tumbling suspension of active rod-like particles. Note that previous numerical calculations of flow fields in steady state in a confined apolar active gel in a slab suggest that non-linear effects are more pronounced in the tumbling

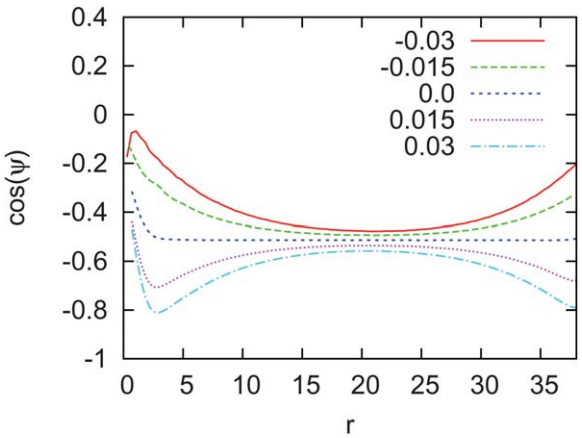

Fig. 4 Value of the cosine of the angle ψ, as a function of the distance from the centre of the active patch (and of the defect), r, for $\zeta = 0.005$, $\lambda = 2.1$, and different values of δK (see legend). As we work on a lattice, the curves plotted are splined averaged interpolation of the angles on the simulated points on the lattice—the average is needed as the function is not exactly isotropic.

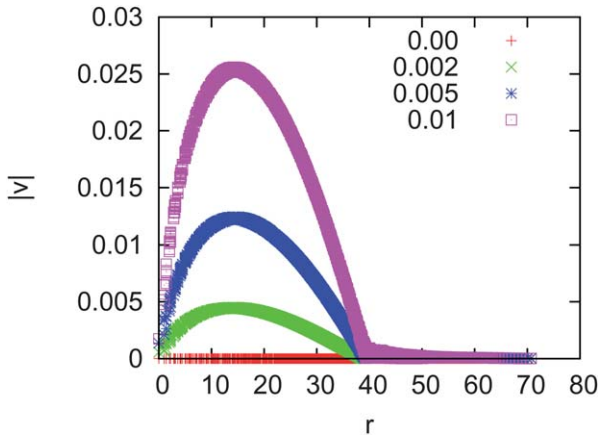

Fig. 5 Plot of the steady state velocity magnitude as a function of the distance from the centre of the active patch (and of the defect), r, for $\delta K = 0$, $\lambda = 2.1$, and different values of ζ (see legend, or, from bottom to top, curves correspond to ζ equal to 0, 0.002, 0.005, 0.01).

regime,[12,29] so that simulations are needed to get a complete picture of the physics for $|\lambda| < 1$.

Fig. 6 shows that also in our case flow-tumbling and flow-aligning materials behave vastly differently. Qualitatively, the most striking difference is that for $0 < \lambda < 1$ it becomes possible to observe non-stationary solutions, such as moving asters which either move out of the active patch or transform into other different structures, some of which are shown as snapshots in Fig. 6. These different structures are clearly dominated by non-linear effects and it would have been very difficult to guess their existence by means of analytical treatments. For extensile fluids, these new non-linear states may be viewed as deformed vortices, with additional splay-bend deformations; for extensile fluids, they may be described as highly distorted asters. Note that the additional deformation does not however lead to more defects. Finally, it should be highlighted that the value of $\cos(\psi)$ for

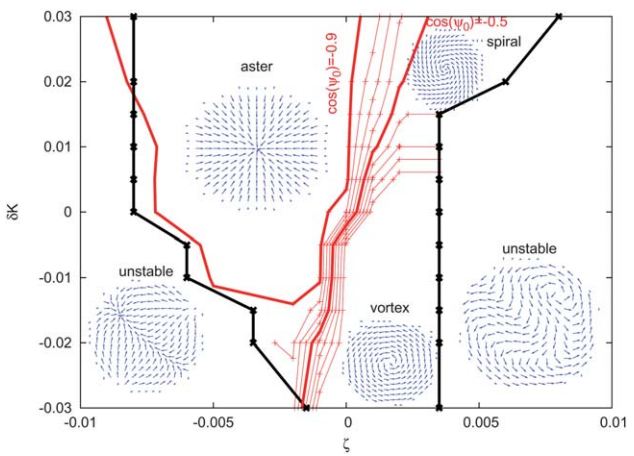

Fig. 6 Phase diagram with $\lambda = 0.7$, and other parameters as in Fig. 1. Red lines denote contour lines of $\cos\psi_0$—starting from the thick line at $\cos\psi_0 = -0.9$, and moving in a clockwise direction the red lines correspond to $\cos\psi_0$ equal to -0.8, -0.7, -0.6 (thin lines), -0.5 (thick), -0.4, -0.3, -0.2, -0.1 (thin). Black lines mark boundaries between stationary and non-stationary states (labelled unstable) at late times.

flow-tumbling active fluids is strongly non-uniform, especially in the non-linear regimes of high $|\zeta|$—more work may be needed to accurately characterise these parameter space regions.

3.1.2 Role of self-advection. We now turn to the case in which the self-advection term w is switched on. Such a term differentiates in our continuum theory "shakers" from "movers", in the terminology of ref. 1. For simplicity we focus here on positive values of w (see eqn (1)). Two of the resulting phase diagrams are shown in Fig. 7.

For small values of self-advection (see Fig. 7, top), we find that the vortex phase increases slightly in size with respect to the apolar case. This is presumably because a pure vortex is invariant under self-advection, (as the order parameter can advect itself around the concentric circles characterising the vortex) so that this is a solution of the polar equations of motion. For larger values of the polar active term, we instead find that the dominant effect is to end up, for most choices of the parameters, with an

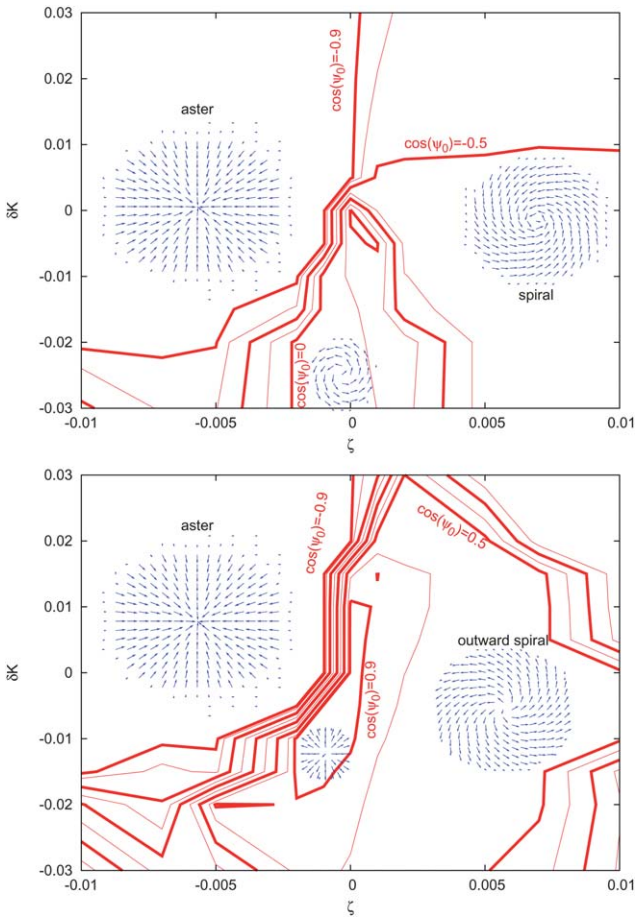

Fig. 7 Phase diagrams with $\lambda = 2.1$ and two values of the self-advection parameter, $w = 0.001$ (top) and $w = 0.005$ (bottom). Red lines denote contour lines of $\cos\psi_0$. In the top panel starting from the thick line at $\cos\psi_0 = -0.9$, and moving in a clockwise direction the red lines correspond to $\cos\psi_0$ equal to -0.7 (thin line), -0.5 (thick), -0.25 (thin), 0 (thick), 0.25 (thin), 0.5 (thick). In the bottom panel starting from the thick line at $\cos\psi_0 = -0.9$, and moving in a clockwise direction the red lines correspond to $\cos\psi_0$ equal to -0.7 (thin line), -0.5 (thick), -0.25 (thin), 0 (thick), 0.25 (thin), 0.5 (thick), 0.7 (thin) and 0.9 (thick).

outward spiral (unlike the inward ones found thus far), whereas the vortex phase has now essentially disappeared. Note that while in the apolar case the physics of the system is invariant for a global $\mathbf{P} \rightarrow -\mathbf{P}$ transformation, this is not the case when self-advection is included, so that inwards and outwards pointing defects are now distinguishable, and can be selected by, for instance, changing the sign and magnitude of w.

Given the observed abrupt transition/crossover from inward to outward pointing spirals upon increasing the value of w for contractile fluids, it is interesting to ask what happens in this case if the director is anchored rather than free at the surface of the active patch. Indeed in many active gels, the director field is better modelled as fixed on some appropriate boundaries. For instance, in microtubular networks with molecular motors, which are contractile, the director field describing the fiber orientation should point inwards far from the centre of an aster. Motivated by this observation, we have also explored the role of boundary conditions in the outward aster–inward aster transition found above. In particular Fig. 8 shows the steady state obtained with normal and inward anchoring at the patch boundary. It can be seen that there is now a conflict between the effect of w and the anchoring which is resolved *via* coexistence of outwards and inward pointing asters, which deform into spirals in order to connect to each other. Our results therefore suggest that boundary conditions can play a crucial role in determining the steady director profile and flow patterns in active fluids with defects in them.

3.2 Defect–defect interactions: extensile and contractile fluids

Having described the single defect case, which as demonstrated above already shows a very rich and partially unexpected behaviour, we now turn to the analysis of defect–defect interactions in active fluids. The simplest case, to which we restrict ourselves here, is the one in which we place two defects in the same active patch. We chose to start initially with two asters, one pointing inwards and the other one pointing outwards. In the case of a passive nematic fluid, inwards and outwards pointing defects are indistinguishable, and each of these has topological charge +1. Therefore the defects would not annihilate, rather for the case $\delta K = -0.02$, considered here, in the passive system the asters first turn into spirals and then leave the active region.

We consider first the case of two asters in a contractile fluid. We have simulated the dynamics in an active patch of radius $R = 40$ and with different initial aster separations, d. When $d = 20$ and $\zeta = -0.01$, the two asters repel each other, and reach a steady state with a distance of about 30 (in simulation units, see Fig. 9). This stable distance is also found with $d = 50$, but seems to increase as ζ aproaches 0. On the other hand, if $\zeta > -0.002$ and $d = 50$ one defect moves out. Therefore we find that contractility stabilises the asters even in a situation in which thermodynamically vortices would be preferred at zero activity, in line with the results found in the previous section for the single defect case. Furthermore, in the active case the defects can coexist in the sample even in steady state, and do not migrate out of the system, although this depends on the initial condition.

The extensile case gives rise to an even more interesting behaviour. Fig. 10 shows one snapshot of the dynamics, which may be seen in full in Movie 1 in the ESI.† For $\zeta = 0.002$, and $d = 20$, the asters quickly turn into two rotating spirals (once more as expected from our phase diagram in Fig. 2), and these continuously rotate around each other, yielding a final state where this rotation seemingly continues forever at an approximately constant rotational velocity. This perpetual rotation occurs *via* spontaneous symmetry breaking and can in principle proceed in either direction. It is interesting to note that once the

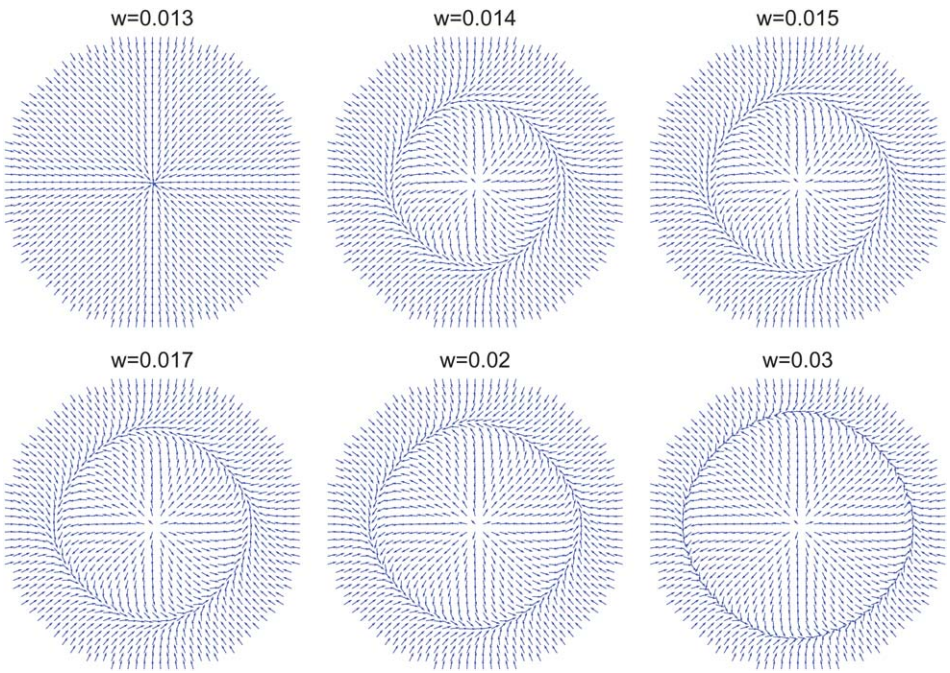

Fig. 8 Plot of the steady state director profile in a system with strong anchoring at the boundary of the active patch, normal to the boundary and pointing inwards. We considered an active patch with $R = 50$ and $\zeta = -0.002$.

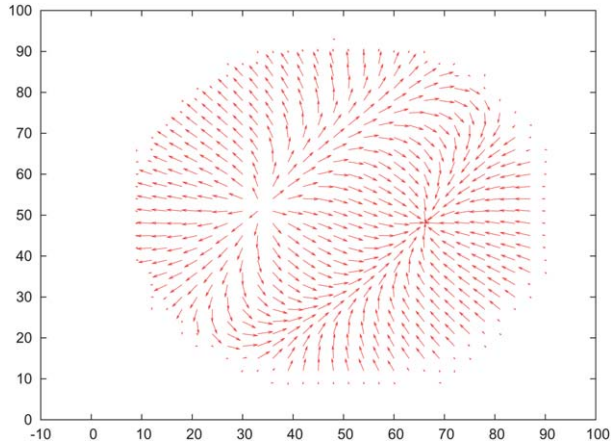

Fig. 9 Steady state obtained from a simulation initialised with two asters, pointing in opposite directions, and originally at a distance of $d = 20$ lattice sites. The radius of the active patch is $R = 40$ (lattice sites). Other parameters are as in Fig. 2, except for $\delta K = -0.02$ and $\zeta = -0.01$.

rotating state is set up, the two spirals are not any more mirror images, rather one is much closer to a vortex than the other one. This asymmetry is maintained indefinitely.

It would be interesting to see whether this behaviour may be quantitatively understood from a theoretical analysis of the equations of motion. From a symmetry point of view, we may understand this perpetually rotating couplet as follows. Each of the spirals may be viewed as an active rotator, with the active gel in between them acting as a medium which hydrodynamically couples these rotators. It is known from simulations and theory of active rotators[30] that pairs may rotate in steady state, therefore what we are seeing may be viewed as an analogous phenomenon.

The angular velocity of the rotation first increases with ζ. However, for $\zeta = 0.005$, we instead observe a different, oscillatory behaviour, where half a clockwise rotation is followed by half an anticlockwise one, and so on. This oscillatory dynamic is shown in Movie 2 in the ESI.† This time the vortex and the spiral defects transform into one another when the sense of the rotation switches from clockwise to anti-clockwise and vice-versa. Finally, for even larger values of the activity, $\zeta = 0.007$, the oscillations becomes less regular and aperiodic, with the initial points of each clockwise or anticlockwise rotation not coinciding anymore. This is consistent with 2D simulations of spontaneous flow in extensile active fluids, where the dynamics becomes seemingly chaotic or turbulent for large enough ζ.[24,29]

Simulations with a different, larger, initial defect–defect separation have shown that there are even more possible steady states in this intriguing 2-defect system. When the initial asters are more separated, $d = 50$, these again turn into spirals but still feel a repulsion which is enough to make them drift away from the active region. What is left after this happens is a defect-free sample, with elastic distortions which do not always disappear and may lead to a spontaneous rotation of the whole droplet, *e.g.* for $\zeta = 0.007$. One shapshot of the director field in such a steady state is shown in Fig. 11, whereas the dynamics are shown in Movie 3 in the ESI.† The director in the centre of the droplet rotates in a clockwise direction in the simulation corresponding to Fig. 11.

4 Discussion and conclusions

In conclusion we have presented here a systematic evaluation of the "phase diagram" of defects in polar active fluids (active gels), in two dimensions. As the order parameter is a polar vector, the most stable defects have topological charge ± 1, in contrast with the apolar nematic case which supports charge $\pm 1/2$. We have focused on the case of charge +1, in line with the previous literature on active gels. In agreement with previous analytical treatments,[4] we have found that asters and vortices are not the only two stable topological defects, but there is a large region of parameter space where spontaneously rotating spirals are selected in steady state.

The hydrodynamics of contractile active fluids have by now often been used as a first approximation to describe cytoskeletal gels and cell extracts.[4,20,21] As such, the best model systems to study are *in vitro* ones, where most of the complications found *in vivo*, such as the presence of a protein regulatory network, the continuous regulated polymerisation and depolymerisation *etc.*,

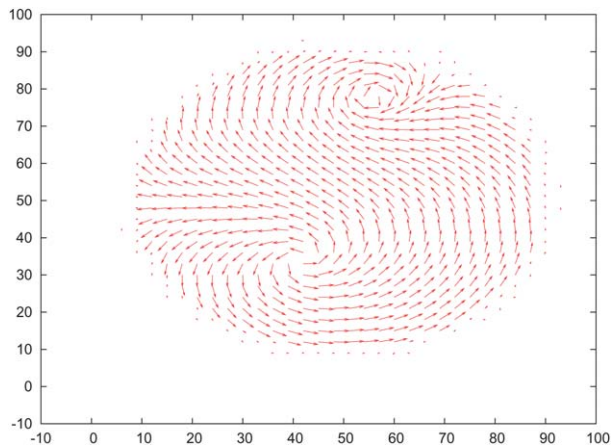

Fig. 10 Snapshot of the director field profile during the steady rotation of the defects which can be observed for parameters as in Fig. 9, except for $\zeta = 0.002$.

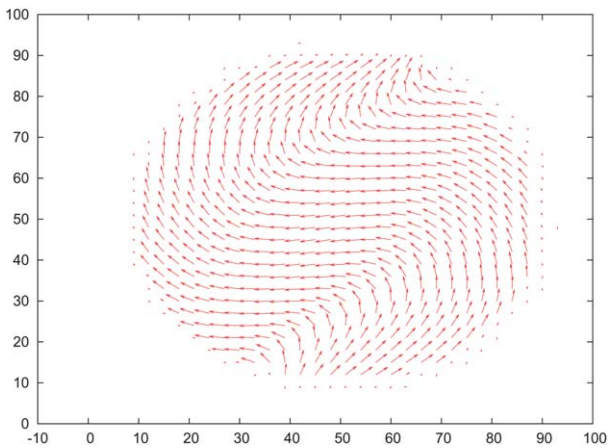

Fig. 11 Snapshot of the director profile for a rotating droplet formed in an initially 2-defect simulation, with $d = 50$. Parameters are as in Fig. 10 except for $\zeta = 0.007$.

are avoided. An exemplar case is given by the *in vitro* experiments by Nedelec *et al.*, documenting the self-assembly of microtubules and kinesin into asters and rotating spirals. As microtubules, like actin fibers, are rod-like (typically flow-aligning) materials,[31] the relevant phase diagrams are those shown in Fig. 2 and Fig. 7. Furthermore, the activity comes from kinesin motors or oligomers which bind to and walk on different filaments, and the resulting forces exerted on the microtubule network are contractile.[4,1] Finally, the values of the elastic constants of active microtubule–kinesin networks are not systematically measured, but if we take typical passive liquid crystalline values, we would argue that the common situation is to have a larger bend elastic constant, *i.e.* $\delta K > 0$. In the resulting parameter region, the hydrodynamic equations of motion for active fluids always predict that asters are the stable topology for defects, and one should not observe spirals, which on the other hand clearly appear in experiments.[32,33]

If spirals are indeed stable, one way to explain this apparent discrepancy with the continuum theory would be that the effective δK is actually negative for active systems. Indeed it is already documented that semiflexible polymers such as actin fibers bend much more than expected from equilibrium thermodynamics in active environments including motors, such as in the cell.[34] Furthermore, the splay elastic constant should diverge in the limit in which the length of the liquid crystalline molecules (microtubules or actin fibers) becomes infinite.[35] However, a quantitative study of this possible effect is thus far missing. A second possibility is that polarity plays an important role. In our model, this would enter through the self-advection term. As can be seen in Fig. 7, and as commented above, for active contractile systems, increasing the magnitude of w decreases the region of stability of asters, and may lead to spirals in steady state, especially when anchoring conditions are applied (see Fig. 8). In both these cases, one would conclude that hydrodynamics may not be needed to lead to steady state spirals. On the other hand, flow is obviously important to get a complete description as the spirals rotate.

Lee and Kardar, and Sankararaman *et al.* studied a non-hydrodynamic model for a microtubular polar order parameter coupled to a concentration field of molecular motors.[36,37] Physically, the couplings are such that the motors walk on microtubules, and also induce local ordering (alignment) of the network. These two couplings were found to be enough to lead to asters,[36,37] but not in general spirals. The latter could on the other hand be obtained when a different coupling between gradient concentration and polarisation was introduced, together with strong anchoring of the polarisation at the boundaries.[37] This purely polar coupling is similar in spirit to our self-advection term in our constant-density hydrodynamic model, and we believe these results lend further credibility to the idea that spirals are due, in the continuum theory, to polar effects and anchoring in the equations of motion. It would be of interest to test the effect of hydrodynamic and of the ζ-active term on the physics of aster and spiral formation in the framework of the model in ref. 36, 37, but this would entail the extension of our current LB algorithm to study binary fluids one of which is an active fluid. We hope to report on this more complicated and realistic modelling in the future.

Alongside the contractile case, we have found that the hydrodynamics of defects in polar extensile fluids is strikingly rich and non-trivial. The physical system of interest is in this case, for instance, a bacterial suspension. We have found that also in this case one should expect to observe, in concentrated suspensions in a confined region, spiral rotating defects. Defect–defect interactions should also lead to a spectacular dynamics. For instance, our simulations show that two defects may (i) perpetually rotate, (ii) oscillate around each other either regularly or irregularly and (iii) leave the system to yield a spontaneously distorted and rotating droplet. Our results should be relevant for and may be tested with confined microbial suspensions, and they may also be compared with hydrodynamic simulations of concentrated suspensions of concentrated rod-like self-propelled particles (see *e.g.* ref. 38).

We acknowledge J. F. Joanny for useful discussions. This work was funded by EPSRC. We thank the HPC-Europa2 programme for funding of JE's visit to Edinburgh, when part of this work was performed.

References

1 Y. Hatwalne, S. Ramaswamy, M. Rao and R. A. Simha, *Phys. Rev. Lett.*, 2004, **92**, 118101.
2 D. Bray, *Cell movements: from molecules to motility*, Garland Publishing, New York (2000).
3 S. Ramaswamy, *Annu. Rev. Condens. Matter Phys.*, 2010, **1**, 323.
4 K. Kruse, J. F. Joanny, F. Julicher, J. Prost and K. Sekimoto, *Phys. Rev. Lett.*, 2004, **92**, 078101.
5 K. Kruse, J. F. Joanny, F. Julicher, J. Prost and K. Sekimoto, *Eur. Phys. J. E*, 2005, **16**, 5.
6 V. Narayan, S. Ramaswamy and N. Menon, *Science*, 2007, **317**, 105.
7 T. Ishikawa and T. J. Pedley, *Phys. Rev. Lett.*, 2004, **92**, 188301.
8 T. Ishikawa and T. J. Pedley, *Phys. Rev. Lett.*, 2008, **100**, 088103.
9 T. B. Liverpool and M. C. Marchetti, *Europhys. Lett.*, 2005, **69**, 846.
10 L. Giomi, T. B. Liverpool and M. C. Marchetti, *Phys. Rev. Lett.*, 2008, **101**, 198101.
11 L. Giomi, T. B. Liverpool and M. C. Marchetti, *Phys. Rev. E: Stat., Nonlinear, Soft Matter Phys.*, 2010, **81**, 051908.
12 D. Marenduzzo, E. Orlandini and Y. M. Yeomans, *Phys. Rev. Lett.*, 2007, **98**, 118102.
13 R. A. Simha and S. Ramaswamy, *Phys. Rev. Lett.*, 2002, **89**, 058101.
14 C. Dombrowski, L. Cisneros, S. Chatkaew, R. E. Goldstein and J. O. Kessler, *Phys. Rev. Lett.*, 2004, **93**, 098103.
15 A. Sokolov, I. S. Aranson, J. O. Kessler and R. E. Goldstein, *Phys. Rev. Lett.*, 2007, **98**, 158102.
16 L. H. Cisneros, R. Cortez, C. Dombrowski, R. E. Goldstein and J. O. Kessler, *Exp. Fluids*, 2007, **43**, 737.
17 M. E. Cates, S. M. Fielding, D. Marenduzzo, E. Orlandini and J. M. Yeomans, *Phys. Rev. Lett.*, 2008, **101**, 068102.
18 T. B. Liverpool and M. C. Marchetti, *Phys. Rev. Lett.*, 2006, **97**, 268101.
19 A. N. Beris and B. J. Edwards, *Thermodynamics of Flowing Systems*, Oxford University Press, Oxford, (1994).
20 R. Voituriez, J. F. Joanny and J. Prost, *Europhys. Lett.*, 2005, **70**, 404–410.
21 R. Voituriez, J. F. Joanny and J. Prost, *Phys. Rev. Lett.*, 2006, **96**, 028102.
22 A. Zumdiek, R. Voituriez, J. Prost and J. F. Joanny, *Faraday Discuss.*, 2008, **139**, 369–375.
23 S. Succi, *The Lattice Boltzmann Equation for Fluid Dynamics and Beyond*, Oxford University Press (2001).
24 M. E. Cates, O. Henrich, D. Marenduzzo and K. Stratford, *Soft Matter*, 2009, **5**, 3791.
25 A. Tiribocchi, N. Stella, A. Lamura and G. Gonnella, *Phys. Rev. E: Stat., Nonlinear, Soft Matter Phys.*, 2009, **80**, 026701.
26 A. Polimeno, L. Orian, A. F. Martins and A. E. Gomes, *Phys. Rev. E: Stat. Phys., Plasmas, Fluids, Relat. Interdiscip. Top.*, 2000, **62**, 2288.
27 D. Marenduzzo and E. Orlandini, *Soft Matter*, 2010, **6**, 774.
28 S. A. Edwards and J. M. Yeomans, *Europhys. Lett.*, 2009, **85**, 18008.
29 D. Marenduzzo, E. Orlandini, M. E. Cates and J. M. Yeomans, *Phys. Rev. E: Stat., Nonlinear, Soft Matter Phys.*, 2007, **76**, 031921.

30 I. Llopis and I. Pagonabarraga, *Eur. Phys. J. E*, 2008, **26**, 103; M. Leoni and T. B. Liverpool, arXiv:1012.2768.
31 T. Sugiyama, D. Miyashiro, D. Takao, H. Iwamoto, Y. Sugimoto, K. Wakabayashi and S. Kamimura, *Biophys. J.*, 2009, **97**, 3132–3138.
32 F. J. Nedelec, T. Surrey, A. C. Maggs and S. Leibler, *Nature*, 1997, **389**, 305.
33 F. Nedelec, *J. Cell Biol.*, 2002, **158**, 1005.
34 M. L. Gardel, F. Nakamura, J. H. Hartwig, J. C. Crocker, T. P. Stossel and D. A. Weitz, *Proc. Natl. Acad. Sci. U. S. A.*, 2006, **103**, 1762.
35 P. G. de Gennes, *Mol. Cryst. Liq. Cryst.*, 1977, **34**, 177.
36 H. A. Lee and M. Kardar, *Phys. Rev. E: Stat. Phys., Plasmas, Fluids, Relat. Interdiscip. Top.*, 2001, **64**, 056113.
37 S. Sankararaman, G. I. Menon and P. B. S. Kumar, *Phys. Rev. E: Stat., Nonlinear, Soft Matter Phys.*, 2004, **70**, 031905.
38 I. Llopis and I. Pagonabarraga, *Europhys. Lett.*, 2006, **75**, 999.